DOI 10.1007/s10958-024-07056-6
Journal of Mathematical Sciences, Vol. 279, No. 6, March, 2024

SCHEMES OF FINITE ELEMENT METHOD FOR SOLVING MULTIDIMENSIONAL BOUNDARY VALUE PROBLEMS

Balt Batgerel
Mongolian Academy of Sciences
54 B Peace Av., Bayanzurkh District
Ulaanbaatar 13330, Mongolia
batgerel@mas.ac.mn

Sergue I. Vinitsky
Joint Institute for Nuclear Research
6, Joliot-Curie St., Dubna 141980, Russia
Peoples' Friendship University of Russia
6, Miklukho-Maklaya St., Moscow 117198, Russia
vinitsky@theor.jinr.ru

Ochbadrakh Chuluunbaatar*
Joint Institute for Nuclear Research
6, Joliot-Curie St., Dubna 141980, Russia
Mongolian Academy of Sciences
54 B Peace Av., Bayanzurkh District
Ulaanbaatar 13330, Mongolia
Mongolian University of Science
and Technology
34 Baga toiruu, Sukhbaatar District
Ulaanbaatar 14191, Mongolia
chuka@jinr.ru

Jan Buša Jr.
Joint Institute for Nuclear Research
6, Joliot-Curie St., Dubna 141980, Russia
Alikhanyan National Science Laboratory
2, Alikhanyan Brothers St.
Yerevan 0036, Armenia
busa@jinr.ru

Yury A. Blinkov
Chernyshevsky Saratov National Research
State University,
83, Astrakhanskaya St., Saratov 410012, Russia
blinkovua@gmail.com

Alexander A. Gusev
Joint Institute for Nuclear Research
6, Joliot-Curie St., Dubna 141980, Russia
Dubna State University
19, Universitetskaya St., Dubna 141980, Russia
gooseff@jinr.ru

Algirdas Deveikis
Vytautas Magnus University
58 K. Donelaičio
Kaunas LT-44248, Lithuania
algirdas.deveikis@vdu.lt

Galmandakh Chuluunbaatar
Joint Institute for Nuclear Research
6, Joliot-Curie St., Dubna 141980, Russia
Dubna State University
19, Universitetskaya St., Dubna 141980, Russia
chugal@jinr.ru

Vandandoo Ulziibayar
Mongolian University of Science
and Technology
34 Baga toiruu, Sukhbaatar District
Ulaanbaatar 14191, Mongolia
v_ulzii@must.edu.mn

We propose new computational schemes and algorithms of the finite element method for solving elliptic multidimensional boundary value problems with variable coefficients at derivatives in a polyhedral d-dimensional domain, aimed at describing collective models of atomic nuclei. The desired solution is sought in the form of an expansion in the basis of piecewise polynomial functions constructed in an analytical form by joining

* To whom the correspondence should be addressed.

International Mathematical Schools **7**. Mathematical Schools in Mongolia. In Honor of Academician T. Zhanlav

Hermite interpolation polynomials and their derivatives on the boundaries of neighboring finite elements having the form of d-dimensional parallelepipeds. Calculations of the spectrum, quadrupole momentum and electric transitions of standard boundary value problems for the geometric collective model of atomic nuclei are analyzed. Bibliography: 22 *titles. Illustrations*: 5 *figures.*

1 Introduction

The finite element method (FEM) has wide applications in solving elliptic boundary value problems. Despite the long history, especially in the development of the theoretical basis of this method, questions remain open about constructive implementation of the method for rgw numerical solution of multidimensional boundary value problems, which requires additional conditions on the physical parameters or the desired properties of the approximate solutions. In FEM, the desired solution is sought in the form of a basis expansion of piecewise polynomial functions which are typically obtained by joining Lagrange interpolation polynomials [1] and provide the continuous derivatives of the approximate solution only in finite elements, but not on their boundaries, i.e., the solution has only generalized derivatives and belongs to the Sobolev space. When describing boundary value problems with higher derivatives in the theory of elasticity, hydro- and aerodynamics, meteorology, quantum mechanics, the desired approximate solution must be continuous along with its derivatives. When constructing it, instead of the Lagrange interpolation polynomials, Hermite interpolation polynomials [2]–[5] are used.

This paper presents new finite element schemes and algorithms, implemented in the computer algebra systems (CAS) Maple, Mathematica, Matlab and in the Python, C^{++}, Fortran languages for solving multidimensional boundary value problems for elliptic differential equations with variable coefficients at the derivatives describing collective models of atomic nuclei. To reduce a boundary value problem in a polyhedral d-dimensional domain to an algebraic eigenvalue problem, the desired solution is sought as an expansion over the basis of piecewise polynomial functions constructed by joining Hermite interpolation polynomials and their derivatives at the boundaries of adjacent finite elements in the form of d-dimensional parallelepipeds.

At the first stage, the Hermite interpolation polynomials in d variables on a d-dimensional parallelepiped are constructed as the product of d Hermite interpolation polynomials of degree p' for each of the independent variables [6], which are calculated and tabulated in an analytical form [7] by using the recurrence relations in [5, 8] implemented in CAS.

At the second stage, an algorithm is proposed for constructing a basis of linearly independent piecewise polynomial functions in the analytical form from tabulated Hermite interpolation polynomials on a given partition of the polyhedral region d of independent variables into finite elements. For each piecewise polynomial function the algorithm indicates the numbers of Hermite interpolation polynomials on adjacent finite elements by joining which this piecewise polynomial function is obtained and between which the integrals are calculated giving the entries of the stiffness and mass matrices. Using the obtained correspondence, the FEM scheme generates suitable band structures of sparse matrices of stiffness and masses of the algebraic eigenvalue problem which is solved by standard linear algebra procedures.

The performance of the developed finite element schemes, algorithms, and programs implemented in CAS Maple, Mathematica, Matlab and in the Python, C^{++}, Fortran languages is demonstrated by solving benchmark boundary value problems for the five-dimensional anhar-

monic oscillator [9] used in the geometric collective model of atomic nuclei [10, 11]. A comparison of the CPU time of new versions of the developed algorithms and programs depending on the dimension of the resulting algebraic eigenvalue problems is presented by using a conventional personal computer.

The structure of the paper is as follows. Section 2 contains the statement of the d-dimensional boundary value problem and the scheme for solving this problem by using FEM. In this section, we describe the algorithm for constructing the basis of piecewise polynomial functions of d variables in the analytical form and calculating the matrices of the algebraic FEM problem. An illustrative example for $d = 2$ is given. In Section 3, we formulate the boundary value problems and presents examples of the solution to the boundary value problem for the geometric collective model of the five-dimensional anharmonic oscillator by using the FEM scheme with Hermite interpolation polynomials on rectangles. In Conclusion, the results obtained are discussed and prospects are outlined.

2 Boundary Value Problem and Schemes of the Finite Element Method

We consider the self-adjoint boundary value problem for the elliptic differential equation

$$(T + V(x) - E)\Phi(x) = 0, \quad T = -\frac{1}{g_0(x)} \sum_{i,j=1}^{d} \frac{\partial}{\partial x_i} g_{ij}(x) \frac{\partial}{\partial x_j}. \tag{2.1}$$

For the principle part of Equation (2.1) the uniform ellipticity conditions holds in the bounded domain $x = (x_1, \ldots, x_d) \in \Omega$ of the Euclidean space $\mathbb{R}^d$, i.e., there are constants $\mu > 0$ and $\nu > 0$ such that

$$\mu\xi^2 \leqslant \sum_{ij=1}^{d} g_{ij}(x)\xi_i\xi_j \leqslant \nu\xi^2, \quad \xi^2 = \sum_{i=1}^{d} \xi_i^2 \quad \forall \xi_i \in \mathbb{R},$$

where the left inequality expresses the requirement of ellipticity, while the right one expresses the boundedness of the coefficients $g_{ij}(x)$. It is assumed that $g_{ji}(x) = g_{ij}(x)$ and $V(x)$ are real-valued functions, continuous with their generalized derivatives of up to a given order in a bounded polyhedral domain $x = (x_1, \ldots, x_d) \in \overline{\Omega} = \Omega \cup \partial\Omega \in \mathbb{R}^d$ with boundary $S = \partial\Omega$, which ensures the existence of a nontrivial solution $\Phi(x)$, corresponding to the real eigenvalue E and satisfying the Dirichlet and/or Neumann boundary conditions [5].

In FEM, the polyhedral domain

$$\overline{\Omega} = \overline{\Omega}_h(x) = \bigcup_{q=1}^{Q} \Delta_q, \quad \overline{\Omega} \subset \mathbb{R}^d, \tag{2.2}$$

is divided into subdomains Δ_q, called *finite elements*, in each of which the local basis functions $\widehat{\varphi}_{rq}^{\varkappa p'}(x)$, $x \in \mathbb{R}^d$, the Lagrange interpolation polynomials or Hermite interpolation polynomials of degree p' are introduced. Here, we use the multiindex notation, $\varkappa$ determines the derivative order and direction, whereas r is the local number of a node.

The piecewise polynomial functions $N_l^{p'}(x) \in C^{\varkappa^c}$ of degree p' with continuous derivatives of up to a given order are constructed by joining the polynomials $\widehat{\varphi}_{rq}^{\varkappa p'}(x)$ on the finite elements

$\Delta_q \in \overline{\Omega}_h(x)$

$$N_l^{p'}(x) \equiv N_s^{\varkappa p'}(x) = \bigcup_{q=1}^{Q} \{\widehat{\varphi}_{rq}^{\varkappa p'}(x) | x \in \Delta_q\}, \tag{2.3}$$

where l is determined in terms of multiindices $\varkappa = \varkappa_1, \ldots, \varkappa_d$ and $r = r_1, \ldots, r_d$; the node number $s = (s_1, \ldots, s_d)$ is related to the local number r of the same node and the finite element number q. Usually, in FEM with Hermite interpolation polynomials, the piecewise polynomial functions $N_s^{\varkappa p'}(x_{s'})$ satisfy the conditions

$$N_s^{\varkappa p'}(x_{s'}) = \delta_{ss'}\delta_{\varkappa 0}, \quad \frac{\partial^{|\varkappa'|}}{\partial x^{\varkappa'}} N_s^{\varkappa p'}(x)\Big|_{x=x_{s'}} = \delta_{ss'}\delta_{\varkappa\varkappa'}, \quad \frac{\partial^{|\varkappa'|}}{\partial x^{\varkappa'}} = \frac{\partial^{\varkappa'_1}}{\partial x_1^{\varkappa'_1}} \cdots \frac{\partial^{\varkappa'_d}}{\partial x_d^{\varkappa'_d}}.$$

The expansion of the sought solution $\Phi_m^h(x)$ from the Sobolev space $\mathscr{H}_2^{\varkappa^c+1\geqslant 1}(\overline{\Omega})$ in the basis of piecewise polynomial functions $N_l^{p'}(x)$,

$$\Phi_m^h(x) = \sum_{l=1}^{L} N_l^{p'}(x)\Phi_{lm}^h, \tag{2.4}$$

reduces the problem (2.1) to the generalized algebraic eigenvalue problem

$$(\mathbf{A} - \mathbf{B}E_m^h)\mathbf{\Phi}_m^h = 0, \quad (\mathbf{\Phi}_m^h)^T \mathbf{B} \mathbf{\Phi}_m^h = 1, \tag{2.5}$$

with respect to the unknowns E_m^h and $\mathbf{\Phi}_m^h$. The problem (2.5) is solved by standard numerical methods implemented as either built-in procedures, for example, Eigenvector() procedure in Maple, Eigensystem() procedure in Mathematica, eigs() procedure in Matlab, or subroutines in a compilable language, for example, the Python subroutine scipy.linalg.eigh() (see https://docs.scipy.org/doc/scipy/reference/generated/scipy.linalg.eigh.html), the C++ subroutine ARluSymGenEig() (see https://github.com/opencollab/arpack-ng), or the authors' modified version of the Fortran subroutine sspace() [1] for sparse matrices.

The entries of the symmetric $L \times L$-matrices of stiffness $\mathbf{A} = (A_{ll'}^{p'})$ and mass $\mathbf{B} = (B_{ll'}^{p'})$ are the integrals

$$\begin{aligned}
A_{ll'}^{p'} &= \int_\Omega N_l^{p'}(x) N_{l'}^{p'}(x) U(x)\, g_0(x) dx + \sum_{i,j=1}^{d} \int_\Omega \frac{\partial N_l^{p'}(x)}{\partial x_i} \frac{\partial N_{l'}^{p'}(x)}{\partial x_j}\, g_{ij}(x) dx = \sum_{q=1}^{Q} a_{ll'}^{p'q}, \\
a_{ll'}^{p'q} &= \int_{\Delta_q} \widehat{\varphi}_{rq}^{\varkappa p'}(x) \widehat{\varphi}_{r'q}^{\varkappa' p'}(x) U(x)\, g_0(x) dx + \sum_{i,j=1}^{d} \int_{\Delta_q} \frac{\partial \widehat{\varphi}_{rq}^{\varkappa p'}(x)}{\partial x_i} \frac{\partial \widehat{\varphi}_{r'q}^{\varkappa' p'}(x)}{\partial x_j}\, g_{ij}(x) dx, \\
B_{ll'}^{p'} &= \int_\Omega N_l^{p'}(x) N_{l'}^{p'}(x) g_0(x) dx = \sum_{q=1}^{Q} b_{ll'}^{p'q}, \quad b_{ll'}^{p'q} = \int_{\Delta_q} \widehat{\varphi}_{rq}^{\varkappa p'}(x) \widehat{\varphi}_{r'q}^{\varkappa' p'}(x) g_0(x) dx
\end{aligned} \tag{2.6}$$

which are calculated on finite elements $\Delta_q \in \overline{\Omega}_h(x)$ by quadrature formulas of order $p' + 1$.

The estimates for the approximate solution E_m^h, $\Phi_m^h(x) \in \mathscr{H}_2^{\varkappa^c+1\geqslant 1}(\Omega_h)$ with respect to the exact solution E_m, $\Phi_m(x) \in \mathscr{H}_2^2(\Omega)$ are as follows [1]:

$$|E_m - E_m^h| \leqslant c_1 h^{2p'}, \quad \|\Phi_m(x) - \Phi_m^h(x)\|_0 \leqslant c_2 h^{p'+1}, \tag{2.7}$$

where h is the maximum size of the finite element Δ_q, p' is the FEM scheme order, $c_1 > 0$ and $c_2 > 0$ are coefficients independent of h,

$$\|\Phi_m(x)\|_0^2 = \int\limits_{\Omega} g_0(x)\,\Phi_m(x)\Phi_m(x)\,dx. \tag{2.8}$$

The Hermite interpolation polynomials $\widehat{\varphi}_{rq}^{\varkappa p'}(x)$ depending on d variables of the finite element Δ_q shaped as a d-dimensional parallelepiped

$$x = (\overline{x}_1, \ldots, \overline{x}_d) \in [\overline{x}^q_{1;\min}, \overline{x}^q_{1;\max}] \otimes \cdots \otimes [\overline{x}^q_{d;\min}, \overline{x}^q_{d;\max}] = \Delta_q \subset \mathbb{R}^d \tag{2.9}$$

in grids $x_r = (\overline{x}_{1r_1}, \ldots, \overline{x}_{dr_d})$, $r_i = 0, \ldots, p$, $i = 1, \ldots, d$, are defined by the relations [2, 3]:

$$\begin{gathered}\widehat{\varphi}_{rq}^{\varkappa p'}(x_{r'}) = \delta_{r_1 r'_1} \cdots \delta_{r_d r'_d} \delta_{\varkappa_1 0} \cdots \delta_{\varkappa_d 0}, \quad \frac{\partial^{|\varkappa'|}}{\partial x^{\varkappa'}} \widehat{\varphi}_{rq}^{\varkappa p'}(x)\Big|_{x=x_{r'}} = \delta_{r_1 r'_1} \cdots \delta_{r_d r'_d} \delta_{\varkappa_1 \varkappa'_1} \cdots \delta_{\varkappa_d \varkappa'_d}, \\ r = (r_1, \ldots, r_d), \quad \varkappa = (\varkappa_1, \ldots, \varkappa_d), \quad \varkappa_i = 0, \ldots, \varkappa_r^{\max} - 1.\end{gathered} \tag{2.10}$$

The Hermite interpolation polynomials $\widehat{\varphi}_{rq}^{\varkappa p'}(x)$ in d variables are calculated in the analytical form as the product of Hermite interpolation polynomials $\varphi_{r_s q}^{\varkappa_s p'}(\overline{x}_s)$ of degree p' in each variable

$$\widehat{\varphi}_{rq}^{\varkappa p'}(x) = \prod_{s=1}^{d} \varphi_{r_s q}^{\varkappa_s p'}(\overline{x}_s). \tag{2.11}$$

Note that the Hermite interpolation polynomials $\varphi_{rq}^{\varkappa p'}(\overline{x})$ with their derivatives of up to order $(\varkappa_r^{\max} - 1)$ in each variable, which are required for constructing $\widehat{\varphi}_{rq}^{\varkappa p'}(x)$ in (2.11), are determined by (2.10) at $d = 1$. They are calculated and tabulated in advance analytically by means of recurrence relations implemented in CAS [5, 8].

As a known example of such calculation and tabulation, we present the interpolation polynomials $\varphi_{rq}^{\varkappa p'}(\overline{x})$ of degree $p' = 3$ in one variable: the Lagrange interpolation polynomials at $p = 3$ and $\varkappa_{\max} = 1$

$$\begin{aligned}\varphi_{0q}^{03}(\overline{x}) &= -(9/2(\overline{x} - 1/3))(\overline{x} - 2/3)(\overline{x} - 1), \\ \varphi_{1q}^{03}(\overline{x}) &= (27/2)\overline{x}(\overline{x} - 2/3)(\overline{x} - 1), \\ \varphi_{2q}^{03}(\overline{x}) &= -(27/2)\overline{x}(\overline{x} - 1/3)(\overline{x} - 1), \\ \varphi_{3q}^{03}(\overline{x}) &= (9/2)\overline{x}(\overline{x} - 1/3)(\overline{x} - 2/3)\end{aligned} \tag{2.12}$$

and the Hermite interpolation polynomials at $p = 1$ and $\varkappa_{\max} = 2$

$$\begin{aligned}\varphi_{0q}^{03}(\overline{x}) &= (\overline{x} - 1)^2(1 + 2\overline{x}), \\ \varphi_{0q}^{13}(\overline{x}) &= (\overline{x} - 1)^2\overline{x}, \\ \varphi_{1q}^{03}(\overline{x}) &= \overline{x}^2(3 - 2\overline{x}), \\ \varphi_{1q}^{13}(\overline{x}) &= \overline{x}^2(\overline{x} - 1).\end{aligned} \tag{2.13}$$

Figure 1 presents examples of the piecewise polynomial functions (2.3) of two variables $N_l^{p'}(x) = N_l^{p'}(\overline{x}_1, \overline{x}_2) = N_l^{\varkappa_1 \varkappa_2 p'}(\overline{x}_1, \overline{x}_2)$, obtained by joining local functions $\widehat{\varphi}_{r_1 r_2 q}^{\varkappa_1 \varkappa_2 p'}(\overline{x}_1, \overline{x}_2)$,

specified by the product (2.11) of the third degree polynomials $\varphi^{\varkappa p'}_{r_s q_s}(\overline{x}_s)$ in (2.12) and (2.13) in each variable. On the piecewise polynomial functions composed by joining Lagrange interpolation polynomials (in contrast to Hermite interpolation polynomials), one can see sharp bends, which means the discontinuity of the first order derivative.

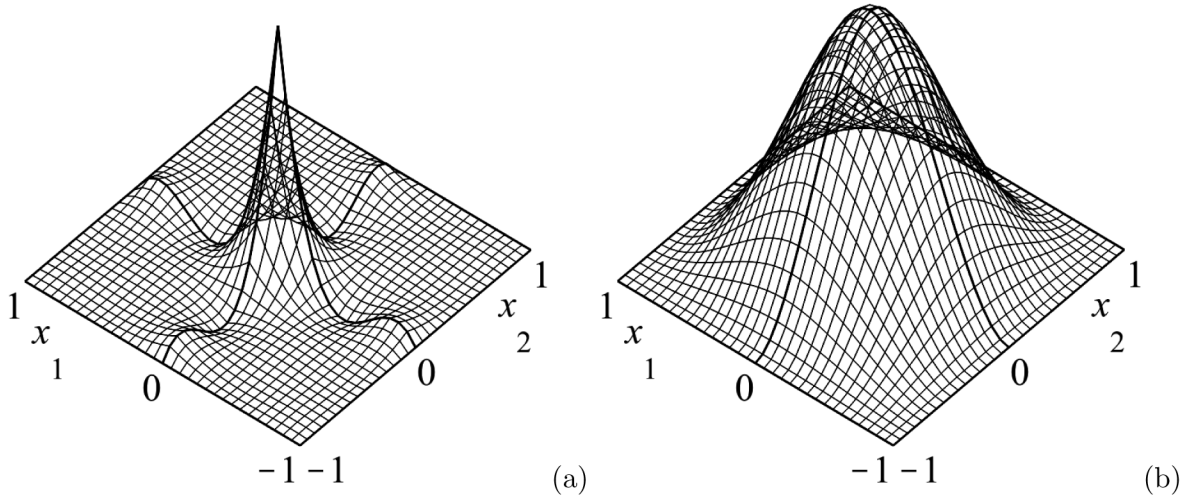

Figure 1. The piecewise polynomial functions $N_l^{\varkappa_1 \varkappa_2 p'}(x_1, x_2)$: (a) $N_{16}^{003}(x_1, x_2)$ and (b) $N_{13}^{003}(x_1, x_2)$ =1 at $(x_1, x_2) = (0, 0)$, composed by joining local functions which are the products of (a) the Lagrange interpolation polynomials and (b) the Hermite interpolation polynomials of the third degree at $Q = 4$.

Let the problem (2.1) be solved on a finite element grid $\overline{\Omega}_h$ defined by (2.2) consisting of parallelepipeds Δ_q defined by (2.9) and, on each of them, specified by the local functions $\widehat{\varphi}^{\varkappa p'}_{rq}(x)$ ordered by the node number $r = (r_1, \ldots, r_d)$, the order and direction of the derivative $\varkappa = (\varkappa_1, \ldots, \varkappa_d)$. The grid nodes are numbered by the global $s = (s_1, \ldots, s_d)$ and local r numbers and the number of the finite element q. For the sake of convenience the local functions $\widehat{\varphi}_t(x) \equiv \widehat{\varphi}^{\varkappa p'}_{rq}(x)$ a re numbered by the global number $t = 1, \ldots, T$. Then the dependence between the set $q, r, \varkappa, s$ and the numbers $l = 1, \ldots, L$ and $t = 1, \ldots, T$ is determined by the algorithm

Algorithm:

- for $q = 1, \ldots, Q$ do
- for all r and $\varkappa$ do
- $t \equiv t(q, r, \varkappa) := t + 1$
- if $\exists q', r', \varkappa'$: $s(q', r') = s(q, r)$ and $\varkappa' = \varkappa$
- then $l \equiv l(q, r, \varkappa) := l(q', r', \varkappa')$
- else $l \equiv l(q, r, \varkappa) := l + 1$
- end if
- end do

We note that the condition in the algorithm is fulfilled only for the nodes enumerated by means of q, r, $\varkappa$ which are at the boundary of the finite elements considered earlier; in this case, the numbers q', r', $\varkappa'$ are known in advance and define the same node, but on the finite element with the minimal number.

As an illustrative example, let us consider the construction of the basis of piecewise polyno-

mial functions (2.3) on the square $[-1,1]\otimes[-1,1]$ divided into $Q=4$ finite elements. Figure 2 shows the correspondence between the index $l=1,\ldots,L$ of the set of basis piecewise polynomial functions $N_l^{p'}(x)$ and the set of indices q, r, $\varkappa$, s characterizing the local functions $\widehat{\varphi}_{rq}^{\varkappa p'}(x)$ ordered by the index $t=1,\ldots,T$: the Lagrange interpolation polynomials of degree $p'=3$ at $p=3$ and $\varkappa_{\max}=1$ at $L=49$ and $T=64$ and the Hermite interpolation polynomials of degree $p'=3$ at $p=1$ and $\varkappa_{\max}=2$ at $L=36$ and $T=64$, which is determined according to Algorithm.

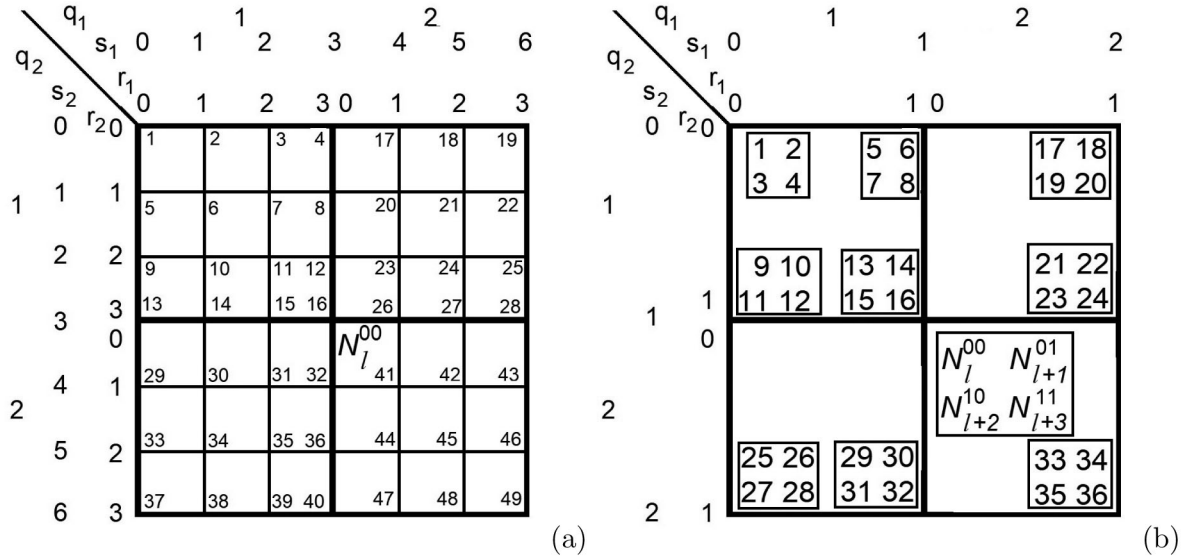

Figure 2. Illustration of constructing the basis of piecewise polynomial functions $N_l^{p'}(x_1,x_2)=N_l^{\varkappa_1\varkappa_2 p'}(x_1,x_2)$, $l=1,\ldots,L$ by joining the local functions $\widehat{\varphi}_{r_1r_2q}^{\varkappa_1\varkappa_2 p'}(x_1,x_2)$ for four ($Q=4$) finite elements Δ_q: (a) Lagrange interpolation polynomials and (b) Hermite interpolation polynomials of the third degree. The heavy lines are the boundaries of finite elements, and the thin lines are zeros of piecewise polynomial functions.

The structures of the $L\times L$-matrices $\mathbf{A}$ or $\mathbf{B}$ in the algebraic problem (2.5) for Lagrange interpolation polynomials and Hermite interpolation polynomials of the third degree on the square $[-1,1]\otimes[-1,1]$ divided into four ($Q=4$) finite elements are shown in Figure 3. Comparing with Figure 2, we see that the indices l and l' of the nonzero entries are related with piecewise polynomial functions containing the local functions on one of the finite elements.

Figure 4 presents the structures of matrices when dividing the square into $Q=3\times 3=9$ and $Q=4\times 4=16$ finite elements and using the piecewise polynomial functions obtained by joining the Hermite interpolation polynomials at $p'=3$. The matrix is divided into 4×4 blocks, because four piecewise polynomial functions correspond to one node, and with an increase in Q the block-banded structure is clearly manifested.

We calculate the FEM integrals (2.6) by the Gauss quadrature formulas of order $p'+1$

$$a_{ll'}^{p'q}=\sum_v G_q^{\varkappa\varkappa'}\Phi_{vrr'\varkappa\varkappa'}U(x_v)\,g_0(x_v)+\sum_v\sum_{i,j=1}^{d}G_{qij}^{\varkappa\varkappa'}\Phi_{vrr'\varkappa\varkappa';ij}\,g_{ij}(x_v),$$
$$b_{ll'}^{p'q}=\sum_v G_q^{\varkappa\varkappa'}\Phi_{vrr'\varkappa\varkappa'q}g_0(x_v), \tag{2.14}$$

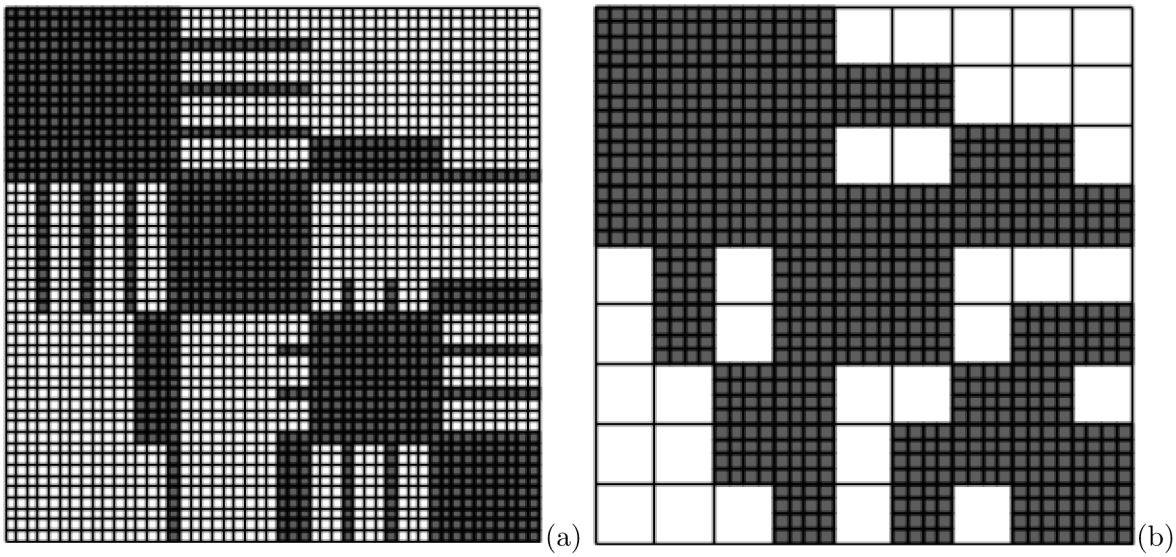

Figure 3. Structures of the $L \times L$-matrices $\mathbf{A}$ and $\mathbf{B}$ (nonzero entries are marked with grey) when using the piecewise polynomial functions constructed by joining the local functions on four ($Q = 4$) finite elements Δ_q: (a) Lagrange interpolation polynomials ($L = 49$) and (b) Hermite interpolation polynomials ($L = 36$) of degree $p' = 3$.

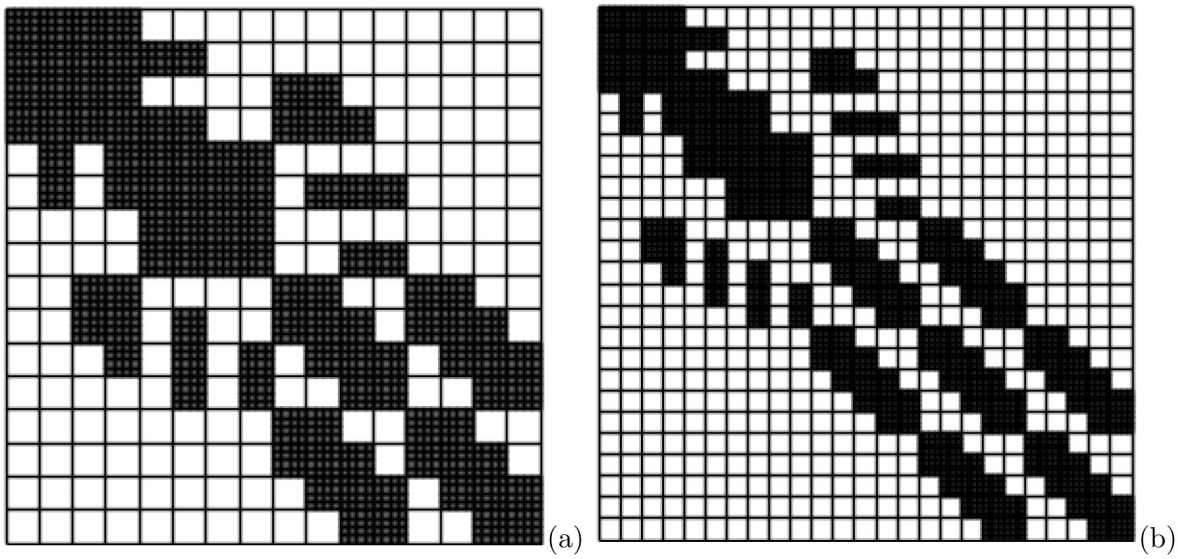

Figure 4. Structure of the $L \times L$-matrices $\mathbf{A}$ and $\mathbf{B}$ for Hermite interpolation polynomials of degree $p' = 3$, $(\varkappa^{\max}, p) = (2, 1)$ on the square $[-1, 1] \otimes [-1, 1]$ divided into (a) $Q = 9$ ($L = 16 \times 4 = 64$) and (b) $Q = 16$ ($L = 25 \times 4 = 100$) finite elements.

$$\Phi_{vrr'\varkappa\varkappa'} = w_v \widehat{\varphi}^{\varkappa p'}_{rq}(y_v) \widehat{\varphi}^{\varkappa' p'}_{r'q}(y_v), \quad \Phi_{vrr'\varkappa\varkappa';ij} = w_v \frac{\partial \widehat{\varphi}^{\varkappa p'}_{rq}(x)}{\partial \overline{x}_i}\bigg|_{y=y_v} \frac{\partial \widehat{\varphi}^{\varkappa' p'}_{r'q}(x)}{\partial \overline{x}_j}\bigg|_{y=y_v}.$$

Here, we use the local coordinates $y = (\overline{y}_1, \ldots, \overline{y}_d) \in [0, 1] \otimes \cdots \otimes [0, 1]$, in Δ_q related to the coordinates (2.9) by $\overline{x}_i = \overline{x}^q_{i;\min} + \overline{y}_i(\overline{x}^q_{i;\max} - \overline{x}^q_{i;\min})$, $i = 1, \ldots, d$, where y_v and x_v are the Gaussian nodes in the local and global coordinates, w_v are the Gaussian weights in the local

coordinates, $G_q^{\varkappa\varkappa'}$ and $G_{qij}^{\varkappa\varkappa'}$ are factors that appear due to the transformation to the local coordinates and for the finite elements on the parallelepiped Δ_q have the form

$$G_q^{\varkappa\varkappa'} = \prod_{u=1}^{d} (\overline{x}_{u;\max}^q - \overline{x}_{u;\min}^q)^{1+\varkappa_u+\varkappa'_u}, \quad G_{qij}^{\varkappa\varkappa'} = \frac{G_q^{\varkappa\varkappa'}}{(\overline{x}_{i;\max}^q - \overline{x}_{i;\min}^q)(\overline{x}_{j;\max}^q - \overline{x}_{j;\min}^q)}.$$

Note that the products $\Phi_{vrr'\varkappa\varkappa'}$ and $\Phi_{vrr'\varkappa\varkappa';ij}$ of the values of the local functions $\widehat{\varphi}_{rq}^{\varkappa p'}(y_v)$ and their derivatives $\dfrac{\partial\widehat{\varphi}_{rq}^{\varkappa p'}(x)}{\partial\overline{x}_i}\Big|_{y=y_v}$ at the Gaussian nodes y_v and with the Gaussian weights w_v were calculated in advance, in contrast to the initial version of the program, and were stored in appropriate arrays, which significantly reduces the time needed to calculate matrices of the algebraic problems.

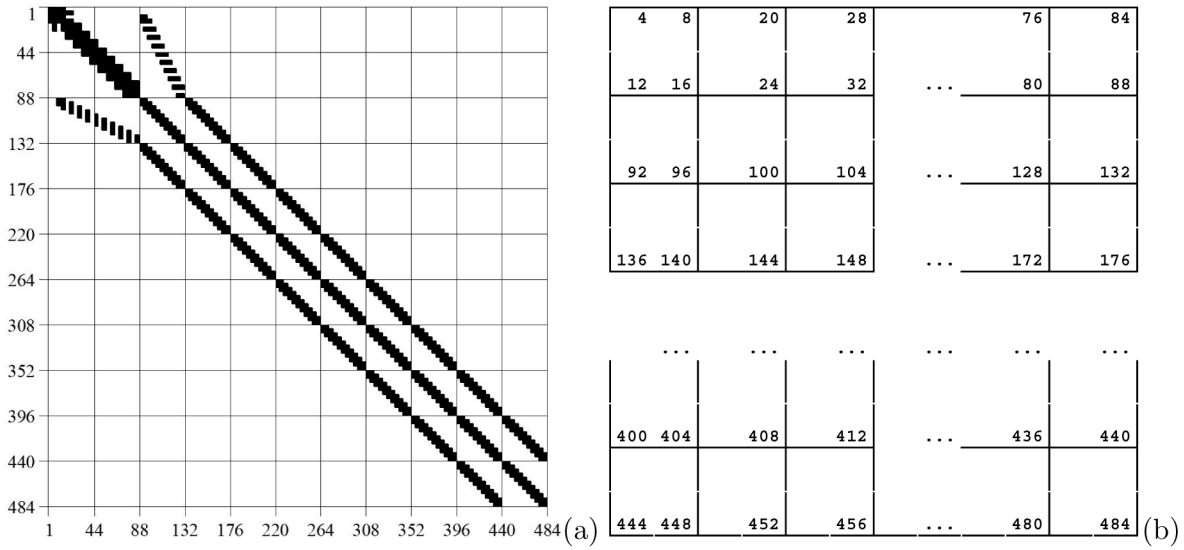

Figure 5. (a) The block-banded structure of the matrices **A** and **B** for Hermite interpolation polynomials of degree $p' = 3$, $(\varkappa^{\max}, p) = (2, 1)$ corresponding to the grid (3.6) for $I = 0$ and the number of finite elements $Q = 10 \times 10 = 100$. (b) Illustration of constructing the basis of piecewise polynomial functions $N_l^{p'}(x_1, x_2) = N_l^{\varkappa_1\varkappa_2 p'}(x_1, x_2)$, $l = 1, \ldots, L = 121 \times 4 = 484$, by joining the local functions $\widehat{\varphi}_{r_1 r_2 q}^{\varkappa_1\varkappa_2 p'}(x_1, x_2)$ for $Q = 100$ finite elements Δ_q. The lines are boundaries of finite elements as in Figure 2, but the numbers l are given only for ones divisible by 4.

3 Boundary Value Problem of Geometric Collective Model

In [11, 12], algebraic versions of the geometric collective model were developed, which were implemented as programs in CAS Mathematica and in the Fortran language for numerical solving the boundary value problem for the five-dimensional anharmonic oscillator with purely discrete spectrum of energy eigenvalues $E_n^I : E_1^I < E_2^I < E_3^I < \cdots$ describing the rotational-vibrational energy bands of atomic nuclei with spin I in the form of an integer angular momentum. Using the expansion of the sought solution of the geometric collective model in the basis functions of the five-dimensional harmonic oscillator with purely discrete, but degenerate spectrum that requires an additional Gram–Schmidt orthogonalization, we can reduce the boundary value

problem to an algebraic eigenvalue problem [9]. The basis functions are parametrized by the internal variables $x_1 = \beta_2, x_2 = \gamma$ and Euler angles $x_3 = \theta_1$, $x_4 = \theta_2$, $x_5 = \theta_3$ in the internal coordinate system and are associated with irreducible representations $U(5) \supset \overline{O(5)} \supset \overline{O(3)}$ of the noncanonical chain of groups [9].

The eigenfunctions $\Psi_n^{IM}(\beta, \gamma, \theta_i)$ of the five-dimensional oscillator of the geometric collective model have the form

$$\Psi_n^{IM}(\beta, \gamma, \theta_i) = \sum_K \Phi_{nK}^I(\beta, \gamma) \mathscr{D}_{MK}^{(I)*}(\theta_i), \tag{3.1}$$

where $\Phi_{nK'}^I(\beta, \gamma)$ are the components, $\mathscr{D}_{MK}^{(I)*}(\theta_i)$ are the orthonormalized Wigner functions

$$\mathscr{D}_{MK}^{(I)*}(\theta_i) = \sqrt{\frac{2I+1}{8\pi^2}} \frac{D_{MK}^{(I)*}(\theta_i) + \widehat{\pi}(-1)^I D_{M,-K}^{(I)*}(\theta_i)}{\sqrt{2(1+\delta_{K0})}},$$

$\widehat{\pi} = \pm 1$ is the parity, $\widehat{\pi} = +1$ for quadrupole deformations ($\widehat{\pi} = -1$ for general deformations [13]), $K = 2 \bmod(I, 2), \ldots, 2\lfloor I/2 \rfloor$.

The boundary value problem for the geometric collective model at fixed integer numbers I and $-I \leqslant M \leqslant I$ reduces to a boundary value problem for a system of two-dimensional partial differential equations, the number of which is equal to $I/2+1$ for even I and $(I-1)/2$ for odd I, coupled by a three-diagonal matrix [10]. Substituting (3.1) into (2.1) and averaging over the basis $\mathscr{D}_{MK}^{(I)*}(\theta_i)$, we obtain an equation for the geometric collective model with respect to the components $\Phi_{nK}^I \equiv \Phi_{nK}^I(\beta, \gamma)$ and eigenvalue E_n^I (MeV) in the form

$$\begin{aligned}
&\sum_{K'} \Big[\Big(T + \frac{2\overline{B}_2}{\hbar^2} (\widehat{V} - E_n^I) \Big) \delta_{KK'} + T_{KK'}^I \Big] \Phi_{nK'}^I = 0, \\
&T = \frac{-1}{\beta^4 \sin(3\gamma)} \Big(\frac{\partial}{\partial \beta} \beta^4 \sin(3\gamma) \frac{\partial}{\partial \beta} + \frac{\partial}{\partial \gamma} \beta^2 \sin(3\gamma) \frac{\partial}{\partial \gamma} \Big), \\
&T_{KK}^I = 2\overline{B}_2 \Big[(I(I+1) - K^2) \Big(\frac{1}{4J_1} + \frac{1}{4J_2} \Big) + \frac{K^2}{2J_3} \Big], \\
&T_{KK'}^I = 2\overline{B}_2 \Big(\frac{1}{8J_1} - \frac{1}{8J_2} \Big) C_{KK'}^I, \quad K' \neq K,
\end{aligned} \tag{3.2}$$

where

$$\begin{aligned}
&C_{KK'}^I = \delta_{K'K-2} C_{KK-2}^I + \delta_{K'K+2} C_{KK+2}^I, \\
&C_{KK-2}^I = (1+\delta_{K2})^{1/2} \times [(I+K)(I-K+1)(I+K-1)(I-K+2)]^{1/2}, \\
&C_{KK+2}^I = (1+\delta_{K0})^{1/2} \times [(I-K)(I+K+1)(I-K-1)(I+K+2)]^{1/2},
\end{aligned}$$

$\overline{B}_2 = 2B_2/\sqrt{5}$ (in 10^{-42} MeV $\cdot$ s $^2 \sim \hbar^2$/MeV) is the mass parameter, β is the dimensionless independent variable, $\hbar = 6.58211828$ (in 10^{-22} MeV $\cdot$ s), and $\widetilde{E} = E 2\overline{B}_2/\hbar^2$ is the dimensionless energy. The moments of inertia are denoted by $J_k = 4\overline{B}_{(k)} \beta^2 \sin^2(\gamma - 2k\pi/3)$, $k = 1, 2, 3$, $\overline{B}_{(k)}$ are the components of the mass tensor along the center-of-mass principal axes of the atomic nucleus, ($\overline{B}_{(k)} = \overline{B}_2$ for the geometric collective model). The potential function of the anharmonic

oscillator $\widehat{V} \equiv \widehat{V}(\beta,\gamma)$ of the geometric collective model is given in the form [11]

$$\widehat{V} = C_2\frac{1}{\sqrt{5}}\beta^2 - C_3\sqrt{\frac{2}{35}}\beta^3\cos(3\gamma) + C_4\frac{1}{5}\beta^4 - C_5\sqrt{\frac{2}{175}}\beta^5\cos(3\gamma)$$
$$+ C_6\frac{2}{35}\beta^6\cos^2(3\gamma) + D_6\frac{1}{5\sqrt{5}}\beta^6. \tag{3.3}$$

The bounded components $\Phi^I_{nK}(\beta,\gamma)$ satisfy the homogeneous Neumann and/or Dirichlet boundary conditions at the boundary points of the intervals $\gamma \in [0,\pi/3]$ and $\beta \in [0,\beta_{\max}]$ and the orthogonality and normalization condition

$$\int\limits_{\beta=0}^{\beta_{\max}}\int\limits_{0}^{\pi/3}\beta^4\sin(3\gamma)\sum_K \Phi^I_{n'K}\Phi^I_{nK}d\gamma d\beta = \delta_{n'n}. \tag{3.4}$$

The boundary value problem for the system of two-dimensional equations (3.2)–(3.4) was solved by means of program 2DFEM, implementing the calculation scheme and algorithm from the above sections using the two-dimensional local functions (2.11) composed of the Hermite interpolation polynomials (2.13). For a test the lower part of the energy spectrum E^I_n of the atomic nucleus ^{190}Os was calculated with the parameters of mass $\overline{B}_2$ and potential $\widehat{V}(\beta,\gamma)$ from [14]:

$$\begin{aligned} &C_2 = -363.64, \quad C_3 = -372.59, \quad C_4 = 19391.8, \quad C_5 = -19246.82, \\ &C_6 = 80003.64, \quad D_6 = -70794.69, \quad \overline{B}_2 = 2/\sqrt{5}\times 173.035. \end{aligned} \tag{3.5}$$

Using the program 2DFEM with the Hermite interpolation polynomial, $p = 1$, $\varkappa_{\max} = 2$, $p' = 3$ the results for 2D boundary value problems (3.2)–(3.4) were obtained on the grid $\Omega^h_{\beta\gamma}$:

$$\Omega^h_{\beta\gamma} = \Omega^h_\beta \otimes \Omega^h_\gamma, \quad \Omega^h_\beta = [0.0, 0.035, \ldots, 0.35], \quad \Omega^h_\gamma = [0, \pi/30, \ldots, \pi/3]. \tag{3.6}$$

Figure 5 shows the structure of the matrices **A** and **B** of the algebraic problem (2.5) corresponding to this grid for $I = 0$ and the number of finite elements $Q = 10\times 10 = 100$ for which the block-banded structure is clearly manifested in comparison with Figure 4. For $I \geqslant 2$ each cell is a $\overline{K}\times\overline{K}$ matrix, where $\overline{K} = I/2+1$ for even I and $\overline{K} = (I-1)/2$ for odd I of the 2D equations (3.2).

Table 1.

procedure/subroutine	type of problem (2.5)	filling the matrices	eigenvalues
Eigenvector()	general	fully populated square	all
Eigensystem()	general	fully populated square	subset
eigs()	general	fully populated square	subset
scipy.linalg.eigh()	complex Hermitian or real symmetric	fully populated lower triangular	subset
ARluSymGenEig()	real symmetric	lower triangular sparse packed storage	subset
sspace()	real symmetric	upper triangular sparse packed storage	subset

Table 2.

I	n	ΔE	band	Exp [14]	TM [7]	TW [7]	TM	TW	TT	TP	TC	TF	$\overline{K}$	$L_{\beta\gamma}$
0	1	0.0	gs 0^+	0.0000	26	26	8	6	0.40	1.25	0.03	0.06	1	484
0	2	1.0427	β 0^+	0.9118										
2	1	0.2485	gs 2^+	0.1867	87	98	16	26	0.42	2.27	0.12	0.14	2	968
2	2	0.7977	γ 2^+	0.5580										
2	3	1.5366	β 2^+	1.1147										
3	1	1.2029	γ 3^+	0.7560	25	24	7	8	0.13	1.08	0.03	0.03	1	484
4	1	0.6060	gs 4^+	0.5479	182	203	36	54	0.73	3.27	0.24	0.27	3	1452
4	2	1.2701	γ 4^+	0.9554										
4	3	1.8141	β 4^+											
5	1	1.7132	γ 5^+	1.2039	84	84	12	13	0.25	1.86	0.12	0.11	2	968
6	1	1.0504	gs 6^+	1.0504	296	325	66	81	1.03	4.16	0.40	0.39	4	1936
6	2	1.7932	γ 6^+	1.4742										
6	3	2.4272	β 6^+											
7	1	2.2832	γ 7^+		169	159	30	22	0.44	2.51	0.24	0.16	3	1452
8	1	1.5663	gs 8^+	1.6665	447	446	118	91	1.26	4.80	0.51	0.47	5	2420
8	2	2.3721	γ 8^+	2.0900										
8	3	3.0806	β 8^+											
9	1	2.9070	γ 9^+		281	257	53	24	0.66	3.16	0.42	0.25	4	1936
10	1	2.1431	gs 10^+	2.3570	624	519	187	67	1.50	5.23	0.74	0.50	6	2904
10	2	3.0034	γ 10^+	2.7720										
10	3	3.7749	β 10^+											

4 Discussion of the Results

To solve elliptic multidimensional boundary value problems with variable coefficients of derivatives, high-precision FEM schemes have been developed with piecewise polynomial basis functions constructed by joining Hermite interpolation polynomials and their derivatives on the boundaries of neighboring finite elements shaped as parallelepipeds.

We describe a new version of the algorithm for constructing d-dimensional basis piecewise polynomial FEM functions in the analytical form, which will be used in the development of software tools in CAS Maple, Mathematica, Matlab and in the Python, C^{++}, Fortran languages for solving multidimensional boundary value problems with variable coefficients at partial derivatives.

Table 1 shows the main differences between the built-in procedures Eigenvector(), Eigensystem(), and eigs() in Maple, Mathematica, and Matlab respectively and library subroutines scipy.linalg.eigh(), ARluSymGenEig(), and sspace() in the Python, C++, and Fortran languages respectively, i.e., type of computed generalized algebraic eigenvalue problem (2.5), matrix fillings, and number of calculated eigenvalues. Note that the subroutine sspace() in Fortran is designed to solve the problem (2.5) with real symmetric block-diagonal (banded) matrices and find the lower part (subset by index) of the eigenvalues; this has been modified by the authors of this paper to the case of sparse matrices. Such an implementation allows us not only to significantly reduce the calculation time, but also makes it possible to solve the problem (2.5) with a significantly higher dimension.

The new version of the algorithm is implemented in the form of the program 2DFEM to

solve the boundary value problem arising in the geometric collective model of atomic nuclei. The efficiency of the developed algorithms and programs is demonstrated by benchmark calculations of the low part of the rotational-vibrational spectrum of the atomic nucleus ^{190}Os presented in Table 2 which demonstrates the high performance of the programs even on a conventional personal computer (PC). Table 2 presents the energy eigenvalues ΔE: $\Delta E_n^I \equiv E_n^I - E_1^0$ (MeV) relative to the energy of the ground state $E_1^0 = -1.0426$ (MeV) for the states of atomic nucleus ^{190}Os with parity $\widehat{\pi} = +1$, calculated by the program 2DFEM of the present paper and ΔE ([7]) calculated by the trial version of the program 2DFEM from [7]. The parameter values of the model (3.5) and the experimental data Exp are taken from [14]. The execution time (CPU) is TM, TW, TT, TP, TC, and TF (seconds) respectively in CAS Maple, Mathematica, Matlab and in the Python, C^{++}, Fortran languages depending on the parameters of the boundary value problems and the corresponding algebraic problems: the nuclear spin I, the number $\overline{K}$ of the 2D equations (3.2), and the dimension $L_{\beta\gamma}$, of eigenvectors of the algebraic problems (2.5).

All calculations were performed using Maple 2023, Mathematica 13, Matlab 2022, Python 3, C^{++}, and Fortran 90 on a PC with AMD Ryzen 9 3950X 16-Core Processor, 3.50 GHz, memory 128 Gb, Windows 10 Pro.

From Table 2 it is clear that the execution time (CPU) TM in Maple and TW in Mathematica of the new 2DFEM program is 3–10 times shorter compared to the time of the trial version of the program from [7]. The time TT in Matlab is much times shorter than TM and TW. We also observe the expected result that the times TC and TF in the compilable languages C++ and Fortran respectively are significantly shorter than the time TP in the compilable Python language.

Table 2 shows the results of calculations of the lower part of the energy spectrum E_n^I by the 2DFEM program that are in a good agreement, with accuracy of 10^{-4} MeV, with calculations of the algebraic version of the fitting geometric collective model for the experimental spectrum [11, 14]. The Runge coefficients

$$r_h = \log_2 \Big| \frac{(E_n^I)_h - (E_n^I)_{h/4}}{(E_n^I)_{h/2} - (E_n^I)_{h/4}} \Big|, \tag{4.1}$$

where $(E_n^I)_h$, $(E_n^I)_{h/2}$, $(E_n^I)_{h/4}$ are the energies calculated by the program 2DFEM in doubly condensed grids, gave estimates $5.29 \div 5.47$, confirming the theoretical estimate (2.7) of order $2p' = 6$.

The results of calculations of quadrupole moments $Q(L, n)$ and electric inter-band and intra-band B(E2) transitions are presented in Appendix.

We emphasize that programs implementing FEM have a significant advantage over the algebraic version of the programs for the geometric collective model that implement the method of expanding the desired solution in the basis functions of a harmonic oscillator with additional variational parameters of mass B_2' and stiffness C_2', since FEM does not have additional variational parameters of piecewise polynomial functions. In addition, the 2DFEM program is applicable to solve a wider class of boundary value problems (2.1), with variable coefficients $g_{ij}(x)$ for derivatives, as well as for parameter values leading to the presence of several minima of potential energy (3.3) as indicated in [7, 14].

The developed approach and programs provide a base for adapting the KANTBP 3.0 program [15] and multidimensional FEM programs for solving the scattering problem [16, 17] and

the problem of bound states of the rotational-vibrational spectrum, which are applicable in various generalizations of the geometric quadrupole collective model [14, 18] and the quadrupole-octupole six-dimensional collective model of atomic nuclei [13, 19]. The FEM program can also be used to study the properties of superheavy nuclei, using the approach proposed in [14].

Table 3.

$Q(L,n)$	present	calc [14]	Exp
$Q(L=2,n=1)$	0.694	0.69	-1.18(3)
$Q(L=4,n=1)$	0.843	0.84	
$Q(L=6,n=1)$	0.885	0.88	
$Q(L=2,n=2)$	-0.643	-0.64	0.9(4)

Table 4.

$L_{\rm gs} \to L_{\rm gs}$	present	calc [14]	Exp
$L_i=0,\ n_i=1 \to L_f=2,\ n_f=1$	1.093	1.09	2.34(6)
$L_i=2,\ n_i=1 \to L_f=4,\ n_f=1$	0.632	0.63	1.12(8)
$L_i=4,\ n_i=1 \to L_f=6,\ n_f=1$	0.636	0.64	1.50(23)
$L_i=6,\ n_i=1 \to L_f=8,\ n_f=1$	0.673	0.67	1.06(6)
$L_\beta \to L_\beta$	present	calc [14]	Exp
$L_i=0,\ n_i=2 \to L_f=2,\ n_f=3$	0.930	0.93	
$L_i=2,\ n_i=3 \to L_f=4,\ n_f=3$	0.022	0.02	
$L_i=4,\ n_i=3 \to L_f=6,\ n_f=3$	0.344	0.34	
$L_i=6,\ n_i=3 \to L_f=8,\ n_f=3$	0.491	0.49	
$L_\gamma \to L_\gamma$	present	calc [14]	Exp
$L_i=2,\ n_i=2 \to L_f=3,\ n_f=1$	0.424	0.42	
$L_i=2,\ n_i=2 \to L_f=4,\ n_f=2$	0.392	0.39	0.70(3)
$L_i=3,\ n_i=1 \to L_f=4,\ n_f=2$	0.114	0.11	
$L_i=3,\ n_i=1 \to L_f=5,\ n_f=1$	0.420	0.42	
$L_i=4,\ n_i=2 \to L_f=5,\ n_f=1$	0.160	0.16	
$L_i=4,\ n_i=2 \to L_f=6,\ n_f=2$	0.510	0.51	0.75(7)
$L_i=5,\ n_i=1 \to L_f=6,\ n_f=2$	0.063	0.06	
$L_i=5,\ n_i=1 \to L_f=7,\ n_f=1$	0.545	0.55	
$L_i=6,\ n_i=2 \to L_f=7,\ n_f=1$	0.088	0.09	
$L_i=6,\ n_i=2 \to L_f=8,\ n_f=2$	0.588	0.59	0.52(15)
$L_i=7,\ n_i=1 \to L_f=8,\ n_f=2$	0.037	0.04	

Table 5.

$L_{\rm gs} \to L_\beta$	present	calc [14]	Exp
$L_i=0,\ n_i=1 \to L_f=2,\ n_f=3$	18.31	18.3	
$L_i=2,\ n_i=1 \to L_f=2,\ n_f=3$	0.36	0.4	
$L_i=2,\ n_i=1 \to L_f=4,\ n_f=3$	0.61	0.6	
$L_i=4,\ n_i=1 \to L_f=4,\ n_f=3$	3.20	3.2	
$L_i=4,\ n_i=1 \to L_f=6,\ n_f=3$	0.47	0.5	
$L_i=6,\ n_i=1 \to L_f=6,\ n_f=3$	2.30	2.3	
$L_i=6,\ n_i=1 \to L_f=8,\ n_f=3$	0.38	0.4	
$L_i=8,\ n_i=1 \to L_f=8,\ n_f=3$	1.71	1.7	

Table 5 (continued).

$L_{\rm gs} \to L_\gamma$	present	calc [14]	Exp
$L_i=0,\ n_i=1 \to L_f=2,\ n_f=2$	81.19	81.2	197(8)
$L_i=2,\ n_i=1 \to L_f=2,\ n_f=2$	201.36	201.4	227(8)
$L_i=2,\ n_i=1 \to L_f=3,\ n_f=1$	43.93	43.9	
$L_i=2,\ n_i=1 \to L_f=4,\ n_f=2$	6.27	6.3	8.2(6)
$L_i=4,\ n_i=1 \to L_f=4,\ n_f=2$	141.80	141.8	229(14)
$L_i=4,\ n_i=1 \to L_f=5,\ n_f=1$	24.04	24.0	
$L_i=4,\ n_i=1 \to L_f=6,\ n_f=2$	2.45	2.5	4.2(40)
$L_i=6,\ n_i=1 \to L_f=6,\ n_f=2$	121.43	121.4	240(6)
$L_i=6,\ n_i=1 \to L_f=7,\ n_f=1$	16.84	16.8	
$L_i=6,\ n_i=1 \to L_f=8,\ n_f=2$	1.52	1.5	
$L_i=8,\ n_i=1 \to L_f=8,\ n_f=2$	109.41	109.4	
$L_\beta \to L_\gamma$	present	calc [14]	Exp
$L_i=2,\ n_i=3 \to L_f=2,\ n_f=2$	16.23	16.2	
$L_i=2,\ n_i=3 \to L_f=4,\ n_f=2$	29.15	37.1	
$L_i=4,\ n_i=3 \to L_f=4,\ n_f=2$	191.67	191.7	
$L_i=4,\ n_i=3 \to L_f=6,\ n_f=2$	1.27	11.7	
$L_i=6,\ n_i=3 \to L_f=6,\ n_f=2$	185.44	185.4	
$L_i=6,\ n_i=3 \to L_f=8,\ n_f=2$	0.25	5.7	
$L_i=8,\ n_i=3 \to L_f=8,\ n_f=2$	171.16	171.1	

A Appendix. Quadrupole Momentum and Electrical Transitions

The electric quadrupole momentum of nuclear levels $Q(L,n)$ and the probabilities of electrical transitions between levels of various bands B(E2) are defined in the laboratory system [20]. Matrix elements of the electric quadrupole operator are evaluated by transforming the operator and collective eigenfunctions into the intrinsic frame. To simplify the formulas below, the reduced matrix elements of the electric quadrupole operator are denoted by

$$\langle \Phi^{L_f}_{n_f} || Q_2 || \Phi^{L_i}_{n_i} \rangle = \sqrt{\frac{2L_i+1}{2L_f+1}} \langle n_f, L_f || \widehat{Q}_{\lambda=2} || n_i, L_i \rangle, \tag{A.1}$$

where Ψ^L_n are eigenfunctions in the laboratory system.

A calculation of the reduced matrix elements of the electric quadrupole operator can be performed within the intrinsic frame as follows:

$$\begin{aligned}\langle n_f, L_f || \widehat{Q}_{\lambda=2} || n_i, L_i \rangle = \sum_{K_i \geqslant 0, \text{even}} \Bigg(& C^{L_f K_f = K_i}_{L_i K_i 20} \int \Phi^{L_i}_{n_i K_i} Q'_{2,0} \Phi^{L_f}_{n_f K_i} d\tau \\ & + \sqrt{1+\delta_{K_i 0}} C^{L_f K_f = K_i + 2}_{L_i K_i 22} \int \Phi^{L_i}_{n_i K_i} Q'_{2,+2} \Phi^{L_f}_{n_f K_f = K_i + 2} d\tau \\ & + \sqrt{1+\delta_{K_i 2}} C^{L_f K_f = K_i - 2}_{L_i K_i 2 -2} \int \Phi^{L_i}_{n_i K_i} Q'_{2,-2} \Phi^{L_f}_{n_f K_f = K_i - 2} d\tau \Bigg),\end{aligned} \tag{A.2}$$

where $K_f = K_i + 2 \leqslant L_f$, $K_f = K_i - 2 \geqslant 0$, $C^{L_f K_f}_{L_i K_i 2K}$ are the Clebsh–Gordan coefficients, and the operator $Q'_{2\mu}$ of electric quadrupole momentum in the intrinsic system (1 b = 100 fm^2) is expressed as

$$\begin{aligned} Q'_{2,0} &= \frac{3ZeR_0^2 10^{-2} b}{4\pi}\Big(\beta\cos(\gamma) + \frac{2}{7}\sqrt{\frac{5}{\pi}}\beta^2\cos(2\gamma)\Big), \\ Q'_{2,\pm 2} &= \frac{3ZeR_0^2 10^{-2} b}{4\pi}\Big(\frac{1}{\sqrt{2}}\beta\sin(\gamma) - \frac{1}{7}\sqrt{\frac{10}{\pi}}\beta^2\sin(2\gamma)\Big), \end{aligned} \tag{A.3}$$

Z is the nucleus charge, $R_0 = 1.1\,A^{1/3}$ fm and A are the nucleus radius and mass.

The matrix element of the electric quadrupole momentum of the operator $Q_{\lambda\mu}$ is expressed in terms of the reduced ones $||Q_\lambda||$ by the Wigner–Eckart formula [21]

$$\langle \Phi^{L_f M_f}_{n_f} | Q_{\lambda\mu} | \Phi^{L_i M_i}_{n_i} \rangle = C^{L_f M_f}_{L_i M_i \lambda\mu} \langle \Phi^{L_f}_{n_f} || Q_\lambda || \Phi^{L_i}_{n_i} \rangle, \tag{A.4}$$

where the factor $(-1)^{2\lambda}(2L_f{+}1)^{-1/2}$ was included in the reduced matrix elements $\langle \Phi^{L_f}_{n_f} || Q_\lambda || \Phi^{L_i}_{n_i} \rangle$ against to the conventional definition [22]. So, the matrix elements of the electric quadrupole momentum (in units eb with factor 10^{-2}) can be written as

$$Q(L_n) = Q_{Ln} = \sqrt{\frac{16\pi}{5}}\langle n, L, M = L | Q_{20} | n, L, M = L \rangle = \sqrt{\frac{16\pi}{5}} C^{LL}_{LL20} \langle Ln || Q_2 || Ln \rangle. \tag{A.5}$$

The electric transitions $B(E\lambda; L_i n_i \to L_i n_i)$ are expressed as the sum of the matrix elements [20]

$$B(E\lambda; L_i n_i \to L_i n_i) = \frac{1}{2L_i + 1} \sum_{M_i M_f \mu} |\langle n_f, L_f, M_f | Q_{\lambda\mu} | n_i, L_i, M_i | \rangle|^2 \tag{A.6}$$

and via the corresponding reduced matrix elements (A.1) or (A.2) (in units e^2b^2 with factor 10^{-4})

$$B(E\lambda; L_i n_i \to L_f n_f) = \frac{2L_f + 1}{2L_i + 1} |\langle n_f, L_f || Q_\lambda || n_i, L_i \rangle|^2 = \langle n_f, L_f || \widehat{Q}_\lambda || n_i, L_i \rangle|^2. \tag{A.7}$$

Thus, to reduce the computer time, we evaluate the lower transitions $B(E\lambda; L_f n_f \to L_i n_i)$ through the calculated upper transitions $B(E\lambda; L_i n_i \to L_f n_f)$ by the formula

$$B(E\lambda; L_f n_f \to L_i n_i) = \frac{2L_i + 1}{2L_f + 1} B(E\lambda; L_i n_i \to L_f n_f). \tag{A.8}$$

Tables 3–5 show the results of calculations of quadrupole moments $Q(L, n)$ in eb units and electric inter-band and intra-band B(E2) transitions in e^2b^2 and $10^3 e^2b^2$ units respectively by the 2DFEM program that are in a good agreement with the calculations [14] for ^{190}Os of the algebraic version of the fitting geometric collective model for experimental data in terms of spectrum, quadrupole momentum, and electrical transitions.

Acknowledgments

The authors thank Professors V. L. Derbov, P. O. Hess and Doctor L. L. Hai for fruitful collaboration.

Funding

The work was financially supported by the Hulubei–Meshcheryakov Joint Institute for Nuclear Research program, the Russian Foundation for Basic Research and the Ministry of Education, Culture, Science and Sports of Mongolia (No. 20-51-44001), the Peoples' Friendship University of Russia (RUDN) Strategic Academic Leadership Program (No. 021934-0-000) and the grant from the Ministry of Education and Science of Mongolia (No. ShuG 2021/137).

Declarations

Data availability This manuscript has no associated data.

Ethical Conduct Not applicable.

Conflicts of interest The authors declare that there is no conflict of interest.

References

1. K. J. Bathe, *Finite Element Procedures in Engineering Analysis*, Prentice-Hall (1982).
2. I. S. Berezin and N. P. Zhidkov, *Computing Methods*, Pergamon Press, Oxford (1965).
3. R. A. Lorentz, *Multivariate Birkhoff interpolation*, Springer, Berlin (1992).
4. F. Lekien and J. Marsden, "Tricubic interpolation in three dimensions," *Int. J. Num. Meth. Eng.* **63**, 455–471 (2005).
5. U. Vandandoo et al, *High-Order Finite Difference and Finite-Element Methods for Solving Some Partial Differential Equations*, Springer, Charm (2024).
6. G. Chuluunbaatar et al, "Construction of multivariate interpolation Hermite polynomials for finite element method," *EPJ Web of Conferences* **226**, Article No. 02007 (2020).
7. A. A. Gusev et al, "Hermite interpolation polynomials on parallelepipeds and FEM applications," *Math. Comput. Sci.* **17**, Article No. 18 (2023).
8. A. A. Gusev et al, "Symbolic-numerical solution of boundary-value problems with self-adjoint second-order differential equation using the finite element method with interpolation Hermite polynomials," *Lect. Notes Comput. Sci.* **8660**, 138–154 (2014)
9. M. Moshinsky and Y. F. Smirnov, *The Harmonic Oscillator in Modern Physics*, Harwood Acad. Publ., Chur (1996).
10. D. Troltenier, J. A. Maruhn, W. Greiner, and P. O. Hess, "A general numerical solution of collective quadrupole surface motion applied to microscopically calculated potential energy surfaces," *Z. Phys. A. Hadrons and Nuclei* **343**, 25–34 (1992).
11. D. Troltenier, J. A. Maruhn, and P. O. Hess, "Numerical application of the geometric collective model," In: *Computational Nuclear Physics. Vol. 1*, pp. 105–128, Springer, Berlin (1991).
12. A. Deveikis et al, "Symbolic-numeric algorithm for calculations in geometric collective model of atomic nuclei," *Lect. Notes Comput. Sci.* **13366**, 103–123 (2022).

13. A. Dobrowolski, K. Mazurek, and A. Góźdź, "Rotational bands in the quadrupole-octupole collective model," *Phys. Rev. C* **97**, 024321, 11 p. (2018).

14. M. J. Ermamatov and P. O. Hess, "Microscopically derived potential energy surfaces from mostly structural considerations," *Ann. Phys.* **37**, 125–158 (2016).

15. A. A. Gusev, O. Chuluunbaatar, S. I. Vinitsky, and A. G. Abrashkevich, "KANTBP 3.0: New version of a program for computing energy levels, reflection and transmission matrices, and corresponding wave functions in the coupled-channel adiabatic approach," *Comput. Phys. Commun.* **185**, 3341–3343 (2014).

16. O. Chuluunbaatar et al, "Solution of quantum mechanical problems using finite element method and parametric basis functions," *Bull. Russ. Acad. Sci., Phys.* **82**, 654–660 (2018).

17. P. M. Krassovitskiy and F. M. Pen'kov, "Features of scattering by a nonspherical potential," *Phys. Part. Nucl.* **53**, 247–250 (2022).

18. E. V. Mardyban, E. A. Kolganova, T. M. Shneidman, and R. V. Jolos, "Evolution of the phenomenologically determined collective potential along the chain of Zr isotopes," *Phys. Rev. C* **105**, Article ID 024321 (2022).

19. A. A. Gusev et al, "Finite element method for solving the collective nuclear model with tetrahedral symmetry," *Acta Phys. Pol. B* **12**, 589–594 (2019).

20. J. M. Eisenberg and W. Greiner, *Nuclear Theory. Vol. 1: Nuclear Models. Collective and Single-Particle Phenomena*, North-Holland, Amsterdam etc. (1970).

21. J. M. Eisenberg and W. Greiner, *Nuclear Theory. Vol. 2: Excitation Mechanisms of Nucleus Electromagnetic and Weak Interactions*, North-Holland, Amsterdam etc. (1970).

22. D. A. Varshalovich, A. N. Moskalev, and V. K. Khersonskii, *Quantum Theory of Angular Momentum*, Nauka, Leningrad (1975); World Scientific Publ. Co., Singapore (1988).

Submitted on November 20, 2023